

# The Effect of Varying Path Properties in Path Steering Tasks

Lei Liu<sup>†</sup> and Robert van Liere<sup>‡</sup>

CWI, Amsterdam, the Netherlands

---

## Abstract

*Path steering is a primitive 3D interaction task that requires the user to navigate through a path of a given length and width. In a previous paper, we have conducted controlled experiments in which users operated a pen input device to steer a cursor through a 3D path subject to fixed path properties, such as path length, width, curvature and orientation. From the experimental data we have derived a model which describes the efficiency of the task. In this paper, we focus on studying the movement velocity of 3D manipulation path steering when one or more path properties vary during the task. We have performed a repeated measures design experiment of 8 scenarios, including a scenario in which all path properties were kept constant, 3 scenarios in which the path width, curvature and orientation varied, 3 scenarios of varying two path properties, and 1 scenario of varying all properties. The analysis of our experimental data indicates that a path of varying orientation or width results in a low average steering velocity. During a continuous steering, the joint where a change in path curvature or orientation takes place also significantly decreases the velocity. In addition, path width and curvature are highly-correlated to the average velocity of a segment, i.e. the wider a segment (or the smaller the path curvature), the larger the average steering velocity on that segment. The results of this work could serve as guidelines for designing higher level interaction techniques and better user interfaces for traditional HCI tasks, e.g. 2D or 3D nested-menu navigation.*

Categories and Subject Descriptors (according to ACM CCS): H.5.1 [Information Interfaces and Presentation]: Multimedia Information Systems—Artificial, augmented, and virtual realities; H.5.2 [Information Interfaces and Presentation]: User Interfaces—User-centered design, Interaction styles

---

## 1. Introduction

Path steering is a primitive 3D interaction task in which a user navigates through a path from a source to a target point as fast as possible. Unlike other 3D interaction tasks, e.g. pointing, steering is a constrained movement in which the user is required to stay within boundaries of the path. The boundaries of the path can be defined by various path properties, such as path width, length, curvature, orientation, etc.

Gaining insight into the effect of varying path properties in steering tasks has great practical significance, since finishing a complete steering task usually involves a change in path properties. For example, navigating through 2D nested menus as shown in Figure 1 requires a user to steer through a

path of 3 segments which are of different path width and orientation, but constant curvature. Understanding of the user's motion on each segment and the joints between segments could serve as guidelines for designing higher level interaction techniques and better user interfaces. In addition, examining the motion under discrete change in path properties is a move towards the study of steering on a general path, as a general 3D path usually has a continuous change in path properties.

In a previous paper [LMvL10], we have modeled path steering as a function of the path properties. Many different width, length, curvature and orientation properties were examined, but each of these properties was not changed in the path. From our experimental data we were able to derive a model which describes the efficiency of the steering task as a relationship between task completion time and the path properties.

---

<sup>†</sup> Lei.Liu@cwi.nl

<sup>‡</sup> Robert.van.Liere@cwi.nl

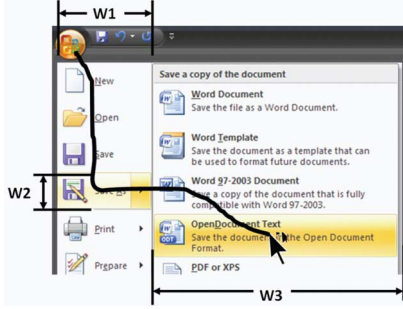


**Figure 1:** A 2D nested-menu task. This is a typical steering task on a path of 3 segments which are of different path width, i.e.  $W1$ ,  $W2$  and  $W3$ , and orientation, i.e. from top to bottom, from left to right and from top to bottom, but the same curvature  $\rho=0$ .

In this paper, we extend our previous work by studying hand-manipulated path steering for paths with varying path properties. We have performed a repeated measures design experiment of 8 scenarios, including a scenario in which all properties were fixed, 3 scenarios of varying only path width, curvature and orientation during a continuous steering, 3 scenarios of varying two of properties and 1 scenario of varying three properties. For the data analysis we qualitatively examine the effect of varying path properties on the average velocity of the movement, but deriving a precise model is beyond the scope of the paper due to the insufficiency of the data. We are also interested in discriminating the average velocities on the joints where path properties vary from those on the segments where no change in path properties takes place.

The contributions of the paper could be summarized as follows:

- We show that the average velocity of a hand-manipulated path steering task is significantly influenced by varying the orientation or width of the path.
- During a continuous steering task, it is shown that there is a significant drop in velocity at the joint where a change in curvature or orientation on the path takes place and the joint where path diverts the most to the decrease in velocity.
- We qualitatively demonstrate that path width significantly influences the average velocity of the segment. The wider a segment, the larger the average steering velocity on that segment.
- Similarly, path curvature also plays a significant role in affecting the average velocity of the segment. The larger the path curvature, the smaller the average steering velocity on that segment.

## 2. Related Work

Unlike pointing task, path steering attracted little attention for years. One exception is the contribution [AZ97, AZ99, AZ01, AZ02, ZAW04] of Accot and Zhai who have been engaged in the study of steering task. They were able to put forward the law of path steering [AZ97, ZAW04], which describes a quantitative relationship between human temporal performance and path spatial properties. Accot and Zhai proposed to consider a path steering task as a set of continuous goal-crossing tasks, each of which could be separately modeled by Fitts' law [Fit54]. If the number of goal-crossing tasks tends to be infinite, the relationship between steering time and the index of difficulty (ID) could be specified in formula 1 below:

$$T_C = a + b \text{ID} = a + b \int_C \frac{ds}{W(s)} \quad (1)$$

where  $a$  and  $b$  are empirically determined constants,  $C$  is a curved path,  $s$  is elementary path length along  $C$  and  $W(s)$  is the path width at path length  $s$ . In the case where path width is constant along the path, the steering law can be rewritten as:

$$T_C = a + b \frac{L}{W} \quad (2)$$

with  $L$  and  $W$  representing the length and width of the path, respectively.

Within the following decade, the steering law has been used to model interactions. For example, Naito, et al. [NKK04] applied the steering law to the study of steering under an environment of "spatially couple style"; Grossman, et al. [GHB\*06] examined the validity of steering law on the Hover-widget-based steering task; Kattinakere, et al. [KGS07] extended the application of steering law to "above-the-surface" layer.

In a previous work [LMvL10], we empirically demonstrated that other path properties could also influence the path steering time besides  $L$  and  $W$ , e.g. path curvature and path orientation. We managed to statistically derive a modified formula as shown in equation 3

$$\log T = a + b \left( \log \frac{L}{W} + c\rho \right) \quad (3)$$

where  $a$ ,  $b$  and  $c$  are experimentally determined constants. ID is redefined as  $\log \frac{L}{W} + c\rho$ , introducing the influence of path curvature ( $\rho$ ), together with length ( $L$ ) and width ( $W$ ). It has also been shown that path orientation could significantly influence the time for steering, though it escaped from a precise modeling.

However, our previous work focused on the total steering time required to navigate through the path, leaving the velocity of the steering aside. In [AZ97], Accot and Zhai also proposed a "local law" that models instantaneous velocity:

$$v(s) = \frac{W(s)}{\tau} \quad (4)$$

where  $\tau$  is an empirically determined time constant. If  $W(s)$  is fixed along the path, equation 4 can be simplified as in:

$$v(s) = \frac{W}{\tau} \quad (5)$$

Formula 5 suggests that the instantaneous velocity is a constant for a path of constant width, resulting in a constant average velocity for the complete task. Note that time and velocity, two ways of describing efficiency of the task, can't be completely independent. Inspired by the previous study on steering time, e.g. formula 3, we believe that formula 5 is not robustly-described, since other path properties, e.g. path curvature or orientation may significantly influence the average velocity of steering as well.

### 3. Experiment

We have designed the *ball and tunnel* task, shown in Figure 2, for the experiment. The users were required to hold an input stylus, represented as a virtual pen bound together with a small cursor ball on tip, to push a virtual target ball through the 3D tunnel. The target ball has exactly the same diameter to that of the circle on the 3D tunnel cross section, making it firmly bound in width. Consequently, the target ball can only move along the tunnel. The boundary of the tunnel is defined as the diameter of the target ball plus two times cursor ball radius, shown in Figure 2.

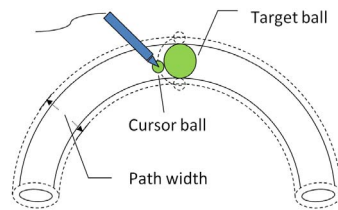


**Figure 2:** *Ball and tunnel task: a cursor ball pushes a target ball through a tunnel. Tunnel width = diameter of target ball; Steering path width = tunnel width + 2 × radius of cursor ball = 2 × (radius of target ball + radius of cursor ball).*

The goal of the task is to push the target ball from one end of the tunnel to the other end as fast as possible. The visual feedback of the target ball is used as a progress indicator for the task. The target ball is movable, defined as steering phase, if the following two requirements are met:

- The cursor ball stays within the boundary of the tunnel;
- The cursor ball is in contact with the target ball.

The steering phase is indicated by a green target ball. Once the cursor ball separates from the target ball or is out of the boundary, the users enter the correction phase in which the target ball remains where it was and turns to red until the users correct for this by returning the cursor ball to the tunnel and continuing the task where they left off. A task starts when the target ball departs from its initial position and terminates when it reaches the end of the tunnel.

### 3.1. Apparatus and Environment

The experiment was performed in a desktop virtual environment (Figure 3), equipped with a PC with high end GPU, a Samsung HL67A750 3D-capable LED DLP HDTV, a pair of Crystal Eyes stereoscopic LCD glasses, a Polhemus FAS-TRAK connected by one 6DOF stylus tracker, and an ultrasound Logitech of 6DOF for head tracking. The resolution of the display was set to  $1920 \times 1080$  @ 120 Hz. The end-to-end latency was measured to be approximately 80ms using the method proposed by Steed [Ste08].



**Figure 3:** *the experimental apparatus: a head tracked stereo display and a 6DOF input stylus.*

As shown in Figure 3, the tunnel was drawn as a semi-transparent 3D tube through which the cursor ball and target ball could easily be seen. To enhance the depth perception, we used the stereoscopic viewing, head tracking, head lighting and a  $0.72\text{m} \times 0.4\text{m} \times 0.4\text{m}$  wire-frame box with a chessboard floor in the virtual world.

The experiment was done in a non-located environment (Figure 4) where the origin of the visual space was 0.4m in front of the display and 0.6 above the desktop, while that of the motor space was set to 1.05m in front of the display and 0.3m above the desktop, respectively. The Control-Display ratio was always set to 1. Subjects were seated 1.35m from the display. They were required not to move their bodies but arms to fulfil a task.

### 3.2. Subjects

Eight right-handed and four left-handed users voluntarily participated in the experiment. There was one female and eleven males, varying in age from 26 to 35. Ten of them had previous experience with virtual environments.

### 3.3. Procedure

As shown in Figure 5, we have conducted a repeated measures design experiment with 8 path types, including a case where no change was applied to the properties of the path, 3 cases where each of the path properties, i.e. path curvature,

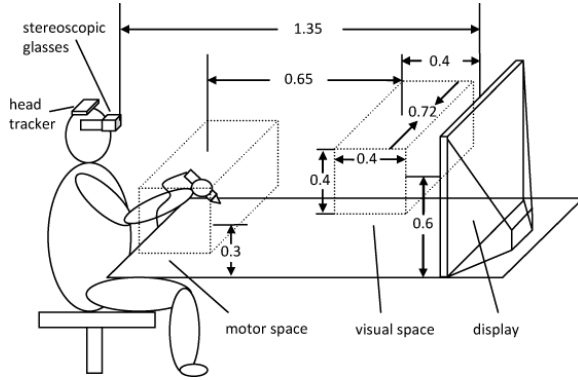


**Figure 4:** the experimental setup [LMvL10] (units: m): Motor and visual space are non-colocated, i.e. there is a horizontal offset of 0.65m and a vertical offset of 0.3m. C-D ratio=1.

width and orientation varied at a time, 3 cases where each combination of 2 properties out of 3 varied and one case where change was applied to all 3 properties.

Curvature is defined as  $\rho = 1/\text{radius}$ , such that a path can be thought of as 3 segments of semicircles of given radius connected up. The first segment was always positioned in xy-plane and, depending on the specific scenarios, other segments might be in xy-, yz- or xz-plane (different orientations). Segments could also have three possible curvatures, i.e.  $8m^{-1}$ ,  $12m^{-1}$  or  $16m^{-1}$ . The radius of the cursor ball was fixed to 0.005m, while that of the target ball might be of 0.010m, 0.015m and 0.020m, resulting in three path widths, i.e. 0.03m, 0.04m and 0.05m, respectively. The properties of a segment on a path were coded in Figure 5, e.g.  $S_1 : \rho 12W0.04P_{xy}$  in scenario (a) indicates segment 1 with a path curvature  $\rho = 12m^{-1}$ , a path width  $W = 0.04m$  and a path orientation in xy-plane. Each of the scenarios was repeated 5 times for a subject, which results in 40 trials per subject. Trials were given in random order which was different from subject to subject.

#### 4. Results

For the repeated measures ANOVA, all data have been normalized to make sure that the observed data distribution is closer to Gaussian distribution.

##### 4.1. Average Velocities between Scenarios

First of all, the average velocity of a trial on the complete path was calculated, resulting in 40 velocities per subject. Then, for each subject, the velocities were separated into 8 groups based on the scenarios, and were further averaged out in each of the groups. Among the 8 scenarios, a repeated measures ANOVA for the average velocities was performed.

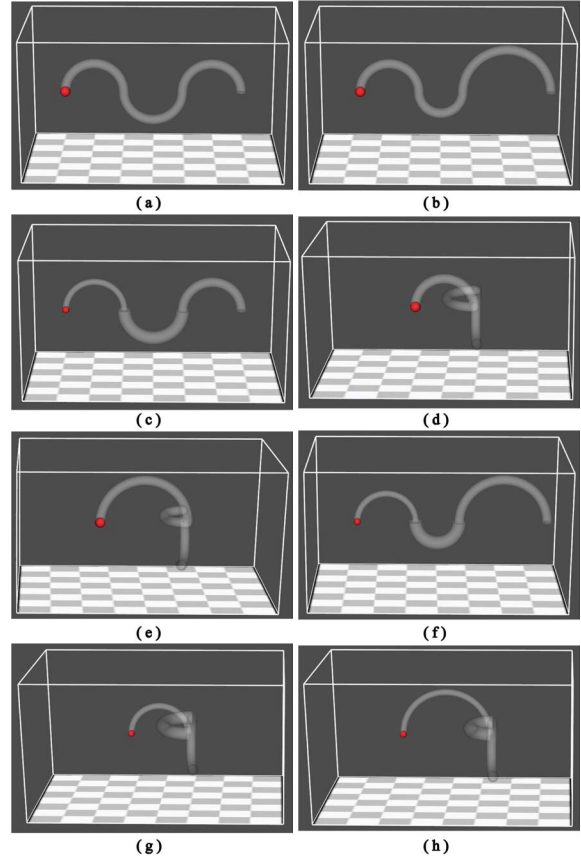


**Figure 5:** 8 scenarios.

- (a). fixed curvature, width and orientation;  
( $S_1, S_2$  and  $S_3 : \rho 12W0.04P_{xy}$ )
- (b). change in curvature;  
( $S_1 : \rho 12W0.04P_{xy}, S_2 : \rho 16W0.04P_{xy}, S_3 : \rho 8W0.04P_{xy}$ )
- (c). change in width;  
( $S_1 : \rho 12W0.03P_{xy}, S_2 : \rho 12W0.05P_{xy}, S_3 : \rho 12W0.04P_{xy}$ )
- (d). change in orientation;  
( $S_1 : \rho 12W0.04P_{xy}, S_2 : \rho 12W0.04P_{xz}, S_3 : \rho 12W0.04P_{yz}$ )
- (e). change in both curvature and orientation;  
( $S_1 : \rho 8W0.04P_{xy}, S_2 : \rho 16W0.04P_{xz}, S_3 : \rho 12W0.04P_{yz}$ )
- (f). change in both curvature and width;  
( $S_1 : \rho 12W0.03P_{xy}, S_2 : \rho 16W0.05P_{xy}, S_3 : \rho 8W0.04P_{xy}$ )
- (g). change in both width and orientation;  
( $S_1 : \rho 12W0.03P_{xy}, S_2 : \rho 12W0.05P_{xz}, S_3 : \rho 12W0.04P_{yz}$ )
- (h). change in curvature, width and orientation.  
( $S_1 : \rho 8W0.03P_{xy}, S_2 : \rho 16W0.05P_{xz}, S_3 : \rho 12W0.04P_{yz}$ )

The corresponding results are illustrated in Figure 6 with the top ends of the columns indicating average velocities of the related scenarios and the error bars representing 95% confidence intervals which were calculated using the method in [ML03].

As shown, there is a statistically significant differ-

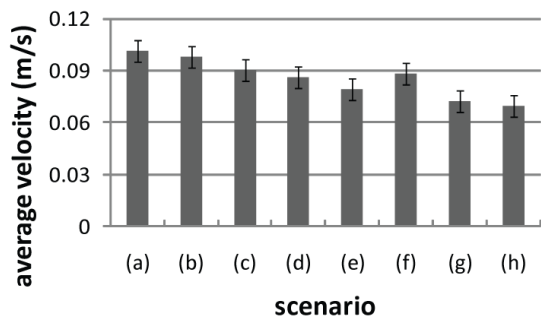


**Figure 6:** The repeated measures ANOVA on the average velocities of 8 scenarios. Scenarios (a)-(h) correspond to those in Figure 5. A significant difference has been found between scenarios.

ence among the average velocities of the 8 scenarios ( $F(7,77)=4.153$ ,  $p=0.0006$ ). The average velocity of scenario (a) serves as a baseline for comparison. The results of scenarios (b)-(d) respectively represent the effect of varying path curvature, width and orientation on average velocities. It can be seen that the change in curvature doesn't significantly influence the average velocities, but those changes in path width and orientation dramatically reduce the average velocities, especially the effect of varying path orientation in scenario (d) which leads to a valley in velocity among the three scenarios. The results of scenarios (e)-(h) are more complex due to the combination of varying two or more path properties at a time. The differences between the average velocities of scenario (a) and each of scenario (e)-(h) are all significant. Scenario (f) remains a relatively high velocity because of the absence of effect of varying path orientation, while the most complex scenario (h) which combines varying all three properties has the largest reduction in velocity among the 8.

#### 4.2. Average Velocities of Segments within Scenarios

A 3D path consists of 3 segments, each of which is a semicircle of a given radius. To examine users' motion on different parts of the path, we further partition the path into 5 segments (see Figure 7), in which  $J_1$  and  $J_2$  describe the joints where two semicircles connect and  $S_1, S_2$  and  $S_3$  are the rest of the segments on each semicircle.  $J_1$  and  $J_2$  are made up of the units on the path whose distance are smaller than  $R=0.04m$  from the joints. In this way, a 3D path can be broken into 3 segments, i.e.  $S_1, S_2$  and  $S_3$  and 2 joints, i.e.  $J_1$  and  $J_2$ .

For the first step, we only focus on the difference between the average velocities on the segments without joints, denoted by  $S$  (see Figure 7) and those with joints, by  $J$ . Figure 8 shows the repeated measures ANOVA results between  $J$  and  $S$  for each of the scenarios.

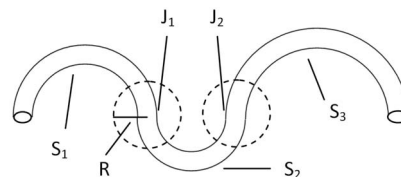


**Figure 7:** Path partition: A 3D path is divided into  $J$  ( $J=J_1+J_2$ ) and  $S$  ( $S=S_1+S_2+S_3$ ).  $J$  doesn't overlap  $S$ .

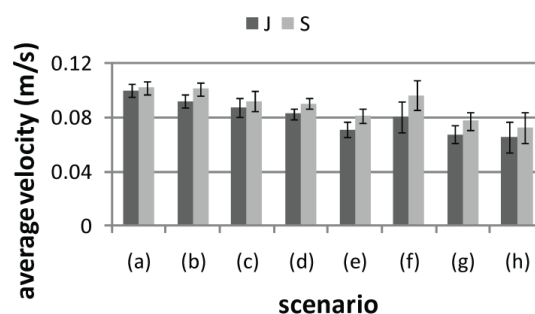


**Figure 8:** The repeated measures ANOVAs on the average velocities of  $J$  and  $S$ . The figure shows 8 independent repeated measures ANOVAs, each of which focuses on the difference between  $J$  and  $S$  in the corresponding scenario. Hence, the confidence intervals between scenarios are not comparable. There is a significant difference in scenarios (b), (d) and (e), respectively.

Statistically, the average velocities of navigating through  $J$  in scenarios (b), (d) and (e) are significantly slower ( $F_b(1,11)=17.452$ ,  $p_b=0.0015$ ;  $F_d(1,11)=6.192$ ,  $p_d=0.0301$ ;  $F_e(1,11)=6.868$ ,  $p_e=0.0237$ ) than that through  $S$ . In scenarios (a), (c), (f), (g) and (h), however, the differences between  $J$  and  $S$  are not significant. Regardless of the statistical significance, the average velocities to navigate through  $J$  are smaller than through  $S$  in all cases.

To further specify the results, we split  $S$  into  $S_1, S_2$  and  $S_3$ , and  $J$  into  $J_1$  and  $J_2$ . A repeated measures ANOVA among  $J_1, J_2, S_1, S_2$  and  $S_3$  for each scenario was done and illustrated in Figure 9. As depicted, there are significant differences among the average velocities of  $J_1, J_2, S_1, S_2$  and  $S_3$  in all scenarios ( $p<0.05$ ), except in scenario (a), the baseline for comparison ( $F(4,44)=1.521$ ,  $p=0.2125$ ). In each of the scenarios, the average velocity on  $J_2$  is always the smallest, compared to those on the corresponding  $J_1, S_1, S_2$  and  $S_3$ , except in scenario (b), while in scenarios (a), (c), (f), (g) and (h), the average velocity on  $S_2$  is the largest. Without taking  $J_1$  and  $J_2$  into account, the velocities on  $S_1, S_2$  and  $S_3$  in (b), (c) and (g) are significantly different from one another.

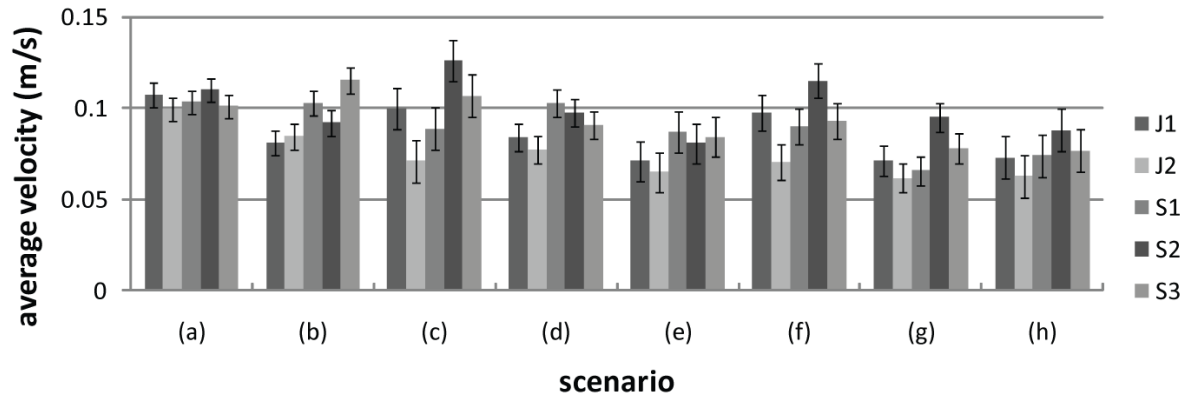


**Figure 9:** 8 repeated measures ANOVA results on the average velocity of  $J_1, J_2, S_1, S_2$  and  $S_3$  in scenarios (a) - (h). The significant difference takes place in scenarios (b) - (h).

## 5. Discussion

In the previous paper [LMvL10], we examined how steering time is influenced by path properties, given scenarios of fixed but different path properties. In this work, however, the focus was switched to the study of average velocity on a certain segment. The reason is that the steering time depends heavily on the segment length crossed, which is not always the same in the 8 scenarios or within the segments (e.g.  $J$  and  $S$ ) of scenarios. The steering velocity, whereas, is not constrained by the segment length but rather represents the difficulty of the same type of segments on a path. The comparison between the average velocities of several segments could easily disclose the difference between the segments. Steering velocity on a segment, together with the time required to steer through the segment, gives a complete description on the efficiency of path steering tasks.

Instead of studying the instantaneous velocity along the path as in [AZ97], in this paper, we focus on the average velocity on a segment (scenario). The reason could be attributed to the variety of the instantaneous velocity during a continuous steering task. Figure 10 shows us a typical velocity profile for a complete path steering task, in which the subject made a correction during the steering on segment  $S_2$ . The fact that the instantaneous velocities oscillate extensively, rather than slightly fluctuate around a constant indicates that Accot and Zhai's local steering law (Equation 4) is substantially not valid for the steering tasks in virtual reality. Due to the intensity of the change, instantaneous velocity can't be used to distinguish between segments (scenarios), while the average velocity on a segment (scenario), in a general sense, represents the characteristic of the segment (scenario).

In the following discussion, we will qualitatively illustrate

the relationship between the path property and the average velocity, but deriving a precise model is beyond the scope of the paper due to the insufficiency of the data. Building up a statistical model by performing a multiple regression analysis usually requires a number of typical values for each of the independent variables. This is apparently not satisfied by the setup of current experiment, as constructing a complicated path with more than 3 widths, curvatures and orientations would dramatically increase the index of difficulty of the task which would consequently lead to a great amount of corrections due to users' fatigue.

### 5.1. Average Velocities between Scenarios

It is worth noting that in Figure 6, scenarios (d), (e), (g) and (h), each of which involves the effect of varying path orientation, rank the slowest 4 among the 8 scenarios. Additionally, all of them have significantly different average velocities from the baseline (a), i.e. the change in path orientation during a 3D path steering task has the most significant influence on the average steering velocity. Similarly, scenarios (c), (f), (g) and (h), influenced by the change in path width, also significantly slower than the baseline, i.e. the change in path width plays a role in affecting the average velocity as well. The fact that scenario (b) which corresponds to the scenario of varying path curvature during the steering is the only scenario that is not significantly different from the baseline illuminates that varying path curvature during a steering task may have the least leverage in average velocity. Generally speaking, the average velocities of the scenarios tend to decline, as the difficulty of the steering task increases (from varying 0 path property to 3).

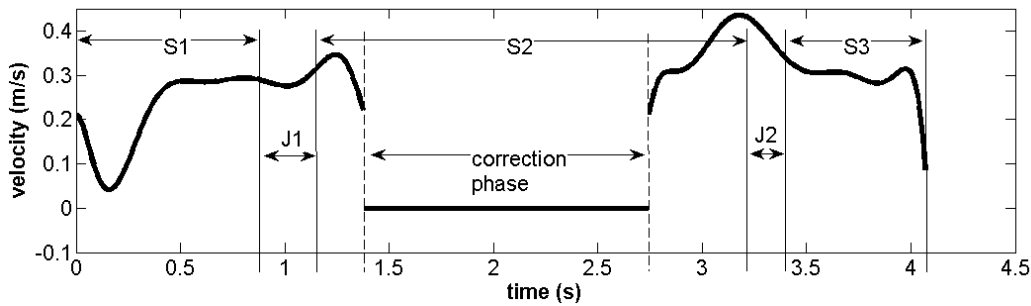


Figure 10: A typical velocity profile for a path steering task.

### 5.2. Average Velocities of J and S within Scenarios

Figure 8 shows that in (b), (d) and (e), the scenarios in which no change has been applied to the path width, the average velocities on  $J$  are always smaller than those on  $S$ . It is clear where there is a change in path curvature or orientation on the path, there is a dramatic reduction in velocity during the joint. However, there tends to be no significant difference between the average velocities of  $J$  and  $S$  if no change appears (scenarios (a),  $p=0.2311$ ) or the path width varies during the steering (scenarios (c), (f), (g) and (h),  $p>0.05$ ). As the average velocity on  $J$  in scenario (d) is significantly smaller than that on the corresponding  $S$ , the slow steering on the joint must contribute the most for the reduction in average velocity of the complete task.

### 5.3. Average Velocities of $S_1, S_2$ and $S_3$ within Scenarios

Leaving  $J_1$  and  $J_2$  behind, we only focus on  $S_1, S_2$  and  $S_3$  at this stage. It is possible to find how the average velocity is influenced by path curvature, width or orientation separately on a certain segment by looking at scenarios (b), (c) and (d) in Figure 9, since in these scenarios only one of the three path properties varies at a time.

In scenario (c), where only the effect of varying path width is present, the average velocities of  $S_1, S_2$  and  $S_3$  are significantly different from each other. Besides, the velocities on each of the segments ( $V_1=0.089\text{m/s}$ ,  $V_2=0.126\text{m/s}$ ,  $V_3=0.107\text{m/s}$ ,  $CI=0.010$ ) relate to the corresponding path widths ( $W_1=0.03\text{m}$ ,  $W_2=0.05\text{m}$ ,  $W_3=0.04\text{m}$ ), i.e. the wider a segment, the larger the average steering velocity on that segment. This specifies that the path width is a key factors influencing the average velocity in path steering tasks, consistent to Accot and Zhai's local steering law in equation 5.

Similarly, scenario (b) in Figure 9 is the case including a single influence of varying path curvature. As shown, significant differences appear between the average velocities of  $S_1, S_2$  and  $S_3$ . Note that the average velocity of  $S_2$  ( $V_2=0.092\text{m/s}$ ) which has the largest curvature ( $\rho_2=16\text{m}^{-1}$ )

is significantly smaller than that of  $S_3$  ( $V_3=0.115\text{m/s}$ ) which has the smallest curvature ( $\rho_3=8\text{m}^{-1}$ ). It illustrates that the path curvature and the corresponding velocity are highly correlated, i.e. the smaller the curvature of a segment, the larger the average steering velocity on that segment. Therefore, it is conclusive that path curvature is another important factors that influences average steering velocity, besides path width.

As evidence shows, however, there is no significant difference between the average velocity of  $S_1, S_2$  and  $S_3$  in scenario (d). The selection of the three orientations in the experiment (on  $xy$ -,  $yz$ - and  $xz$ -plane) may not be the optimal way to demonstrate the effect of varying path orientation so that more data are required to conclude the effect of varying path orientation on the average velocities of the segments with different but fixed orientations.

## 6. Conclusions

In this work, we have examined the manipulation path steering tasks on paths of discrete variable properties, i.e. varying the path curvature, width and orientation during the steering tasks. We have performed a repeated measures design experiment of 8 scenarios, including varying 0, 1, 2 or 3 path properties during a steering task, respectively. The study has focused on the comparison on the average velocities between scenarios and the velocities of segments within a scenario. This work complements the previous work in which the efficiency of the path steering task could only be measured by the time of steering through the complete task.

As the experimental results indicate, the path of varying orientation or width during the steering results in a significant decrease in the average velocity between scenarios. Within a scenario, however, the joint where a change in path curvature or orientation takes place has a low average velocity. Path width and curvature are highly-correlated to the average velocities of the segments without a joint, i.e. the wider a segment (or the smaller the path curvature), the larger the average steering velocity on that segment.

These conclusions provide a better understanding on path steering tasks, which are of great use in guiding the design of user interfaces and higher level interaction techniques. For example, the frequent change in path orientation when navigating through the commonly used 2D nested menus as shown in Figure 1 may undermine the efficiency of the steering, according to the one of the conclusions. This can be solved either by designing a better user interface with fewer sharp turns or by introducing new interaction techniques that can automatically ‘jump’ to the next segment, avoiding the change in steering direction. A future work is needed to substantiate this claim.

## 7. Future Work

Due to the insufficiency of data, as mentioned, a quantitative relationship between path steering velocity and path properties is missing in this work. In addition, the study of path steering on a 3D path with discrete varying path properties is just our first step towards the study of path steering on a general 3D path. More works need to be scheduled to better understand path steering, which could ultimately serve as the guidelines for designing new interaction techniques and user interfaces.

## References

- [AZ97] ACCOT J., ZHAI S.: Beyond Fitts’ law: Models for trajectory-based HCI tasks. In *CHI ’97: Proceedings of the SIGCHI conference on Human factors in computing systems* (1997), pp. 295–302.
- [AZ99] ACCOT J., ZHAI S.: Performance evaluation of input devices in trajectory-based tasks: An application of the steering law. In *CHI ’99: Proceedings of the SIGCHI Conference on Human Factors in Computing Systems* (1999), pp. 466–472.
- [AZ01] ACCOT J., ZHAI S.: Scale effects in steering law tasks. In *CHI ’01: Proceedings of the SIGCHI conference on Human factors in computing systems* (2001), pp. 1–8.
- [AZ02] ACCOT J., ZHAI S.: More than dotting the i’s — foundations for crossing-based interfaces. In *CHI ’02: Proceedings of the SIGCHI Conference on Human Factors in Computing Systems* (2002), pp. 73–80.
- [Fit54] FITTS P. M.: The information capacity of the human motor system in controlling the amplitude of movement. *Journal of Experimental Psychology* 47, 6 (June 1954), 381–391.
- [GHB\*06] GROSSMAN T., HINCKLEY K., BAUDISCH P., AGRAWALA M., BALAKRISHNAN R.: Hover widgets: Using the tracking state to extend the capabilities of pen-operated devices. In *CHI ’06: Proceedings of the SIGCHI conference on Human Factors in computing systems* (2006), pp. 861–870.
- [KGS07] KATTINAKERE R., GROSSMAN T., SUBRAMANIAN S.: Modeling steering within above-the-surface interaction layers. In *CHI ’07: Proceedings of the SIGCHI conference on Human factors in computing systems* (2007), pp. 317–326.
- [LMvL10] LIU L., MARTENS J.-B., VAN LIERE R.: Revisiting path steering for 3D manipulation tasks. In *3DUI’10: Proceedings of the IEEE Symposium on 3D User Interfaces 2010* (2010), pp. 39–46.
- [ML03] MASSON M. E. J., LOFTUS G. R.: Using confidence intervals for graphically based data interpretation. *Canadian Journal of Experimental Psychology* 57, 3 (Sept. 2003), 203–220.
- [NKK04] NAITO S., KITAMURA Y., KISHINO F.: Steering law in an environment of spatially coupled style with matters of pointer size and trajectory width. *Computer Human Interaction 6th Asia Pacific Conference - APCHI 2004 3101* (2004), 305–316.
- [Ste08] STEED A.: A simple method for estimating the latency of interactive, real-time graphics simulations. In *Proceedings of the 2008 ACM symposium on Virtual reality software and technology* (2008), pp. 123–129.
- [ZAW04] ZHAI S., ACCOT J., WOLTJER R.: Human action laws in electronic virtual worlds: An empirical study of path steering performance in VR. *Presence: Teleoperators and Virtual Environments* 13, 2 (2004), 113–127.